Research Paper

Implications of maraviroc and/or rapamycin in a mouse model of fragility

Laura Pérez-Martínez[1], Lourdes Romero[1], Sandra Muñoz-Galván[2,3], Eva M. Verdugo-Sivianes[2,3], Susana Rubio-Mediavilla[4], José A. Oteo[1,5], Amancio Carnero[2,3], José-Ramón Blanco[1,5]

[1]Centro de Investigación Biomédica de La Rioja (CIBIR), Logroño, Spain
[2]Instituto de Biomedicina de Sevilla, IBIS, Hospital Universitario Virgen del Rocío, Universidad de Sevilla, Consejo Superior de Investigaciones Científicas, Sevilla, Spain
[3]CIBERONC, Instituto de Salud Carlos III, Madrid, Spain
[4]Servicio de Anatomía Patológica, Hospital San Pedro, Logroño, Spain
[5]Servicio de Enfermedades Infecciosas, Hospital San Pedro, Logroño, Spain

Correspondence to: José-Ramón Blanco; **email:** jrblanco@riojasalud.es, jrblancoramos@gmail.com
Keywords: CCR5 antagonist, frailty, myostatin, rapamycin
Received: January 29, 2020 **Accepted:** March 31, 2020 **Published:** April 30, 2020

ABSTRACT

Background: As age increases, the risk of developing fragility also increases. Improving the knowledge of frailty could contribute to maintaining the functional ability of elderly people. Interleukin (IL)-10 homozygous knockout mice (IL-10$^{tm/tm}$ [IL10KO]) constitute an excellent tool for the study of frailty. Because patients with frailty demonstrate an overexpression of CCR5, rapamycin (RAPA) and/or maraviroc (MVC), two molecules able to decrease CCR5 expression, were evaluated.

Results: Muscle myostatin was reduced in all the therapeutic groups but the MVC group (p <0.001 for RAPA and MVC-RAPA) and in serum samples (p <0.01 for all the groups). Serum CK levels were also significantly lower in MVC and RAPA groups (p <0.01 in both cases). Lower AST levels were observed in all the therapeutic groups (p <0.05 for all of them). The apoptotic effector caspase-3 was significantly lower in MVC and RAPA groups (p<0.05 in both cases). Combined treatment with MVC-RAPA showed a synergistic increase in p-AKT, p-mTOR and SIRT1 levels.

Conclusions: MVC and RAPA show a protective role in some factors involved in frailty. More studies are needed to prove their clinical applications.

Material and methods: Eighty male homozygous IL10KOs were randomly assigned to one of 4 groups (n= 20): i) IL10KO group (IL10KO); ii) IL10KO receiving MVC in drinking water (MVC group), iii) IL10KO receiving RAPA in drinking water (RAPA group), and finally, iv) MVC-RAPA group that received MVC and RAPA in drinking water. Blood and muscle samples were analysed. Survival analysis, frailty index calculation, and functional assessment were also performed.

INTRODUCTION

Longevity is one of the greatest achievements of modern societies. By 2050 it is estimated that nearly a quarter of the global population will be over 60 years old [1]. As age increases, the risk of developing fragility also increases, suggesting an association between them [2]. Frailty is a syndrome characterized by a state of increasing vulnerability, decreased physical function, and adverse outcomes (mortality, disability, and hospitalization) [3, 4]. The physical phenotype of frailty, described by Fried et al. [4], shows significant overlap with sarcopenia, a progressive and generalized skeletal muscle disorder that involves the accelerated loss of muscle mass and function [5].

Improving the knowledge of frailty could contribute to maintaining the functional ability of elderly people. However, so far, there are many unanswered questions about this syndrome. Because clinical studies of frailty are limited by ethical, logistical, and biological complications, among others, animal models are contributing greatly to our understanding of the biology of aging and have been used to test new potential interventions to enhance survival [6]. Interleukin (IL)-10 homozygous knockout mice (IL-$10^{tm/tm}$ [IL10KO]) [7] are one of these models and constitute an excellent tool for the study of frailty [8]. This is because IL10KO develop several frailty features such as sarcopenia, muscular weakness, weight loss as well an increase in multiple pro-inflammatory cytokines [8].

Increasing evidence suggests that aging is a regulated process, and its course can be modified by the modulation of signal transduction pathways [9]. To date, no specific drugs have been approved for the treatment of frailty but this is a major area of research. Rapamycin (RAPA), a macrolide antibiotic with antiproliferative properties [10], is a specific inhibitor of the mechanistic target of rapamycin (mTOR) pathway [11]. RAPA, not only extended the life span of mice but also has a variety of aging-related conditions in old mice [11–14]. Indeed, RAPA is able to decrease CCR5 mRNA expression [15, 16], which is overexpressed in patients with frailty [17]. In this sense, CCR5 antagonists could also be a therapeutic option for the treatment of frailty. So far, only one specific CCR5 antagonist is currently approved for clinical use, maraviroc (MVC) [18]. At the moment, it is unknown wheter the combination of RAPA plus MVC could have a synergic effect, but a synergic effect was observed with other non-approved CCR5 antagonists [19, 20]. To our knowledge, no study has evaluated the role of MVC and/or RAPA in persons with frailty.

In the current study, our aim was to evaluate the effects of MVC and/or RAPA in an experimental mouse model of frailty.

RESULTS

Survival was similar in all groups

At the end of the experiment all the groups had a similar survival rates. However, there was a trend towards a greater survival in the RAPA group (p=0.072) (Figure 1).

None of the therapeutic interventions reduced body weight

The four groups had a similar baseline weight. At the end of the experiment, no significant differences were observed in the body weights (Figure 1).

All the therapeutic interventions reduced the transaminases

Extra-hepatic sites of aminotransferases include skeletal muscle [31]. For this reason, myocyte injury could raise both AST and ALT [32]. Significant differences in AST levels were observed in favor of all the therapeutic groups: MVC (p=0.023), RAPA (p<0.002) and MVC-RAPA (p<0.001). The analysis of ALT also showed a reduction in all the therapeutic groups, mainly in the MVC-RAPA group (p<0.004) and with a clear tendency in the MVC (p=0.085) and RAPA (p=0.076) groups (Figure 2).

Glucose and insulin parameters were modified in all the groups

Significantly higher serum glucose levels were observed in the MVC-RAPA group (p<0.003). After analyzing the HOMA index, higher levels were observed in the RAPA (p=0.035) and MVC-RAPA (p<0.003) groups (Figure 2). Glucose and insulin tolerance test showed no differences (data not shown).

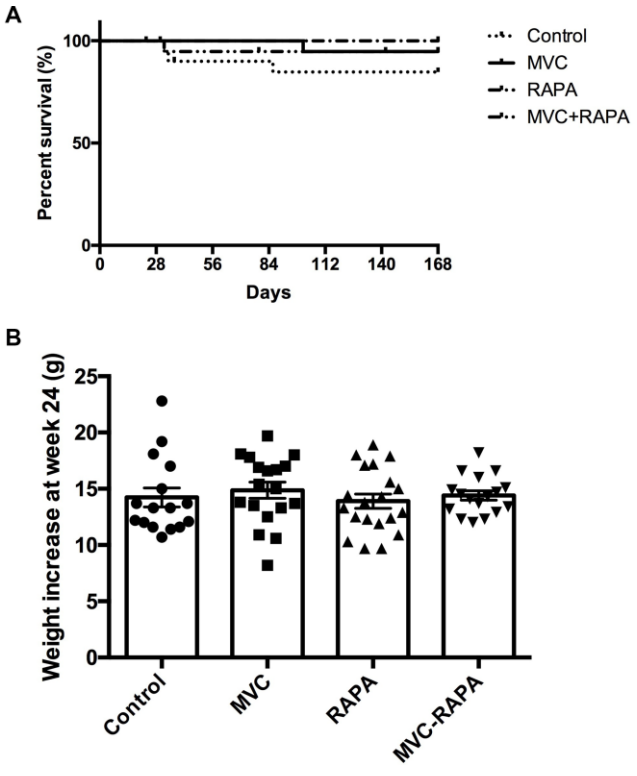

Figure 1. Survival and body weight. (**A**) Kaplan-Meier survival plot shows no differences. (**B**) Weight increase did not show statistically significant differences between groups. Each bar represents the mean ± SEM. *p <0.05 with respect to control. MVC, maraviroc. RAPA, rapamycin. MVC+RAPA, maraviroc plus rapamycin.

The lipid profile of serum TGD improved only in the MVC-RAPA group

No differences were observed after analyzing serum TC levels. Meanwhile, MVC-RAPA groups showed significantly lower levels of serum TGD (p=0.0001) (Figure 2).

None of the therapeutic interventions improved the weight of the quadriceps or gastrocnemius but CK and myostatin levels were improved

Regarding myostatin, its inhibition can induce skeletal muscle hypertrophy, while its overexpression causes muscle atrophy [33]. In our study, all the groups but the

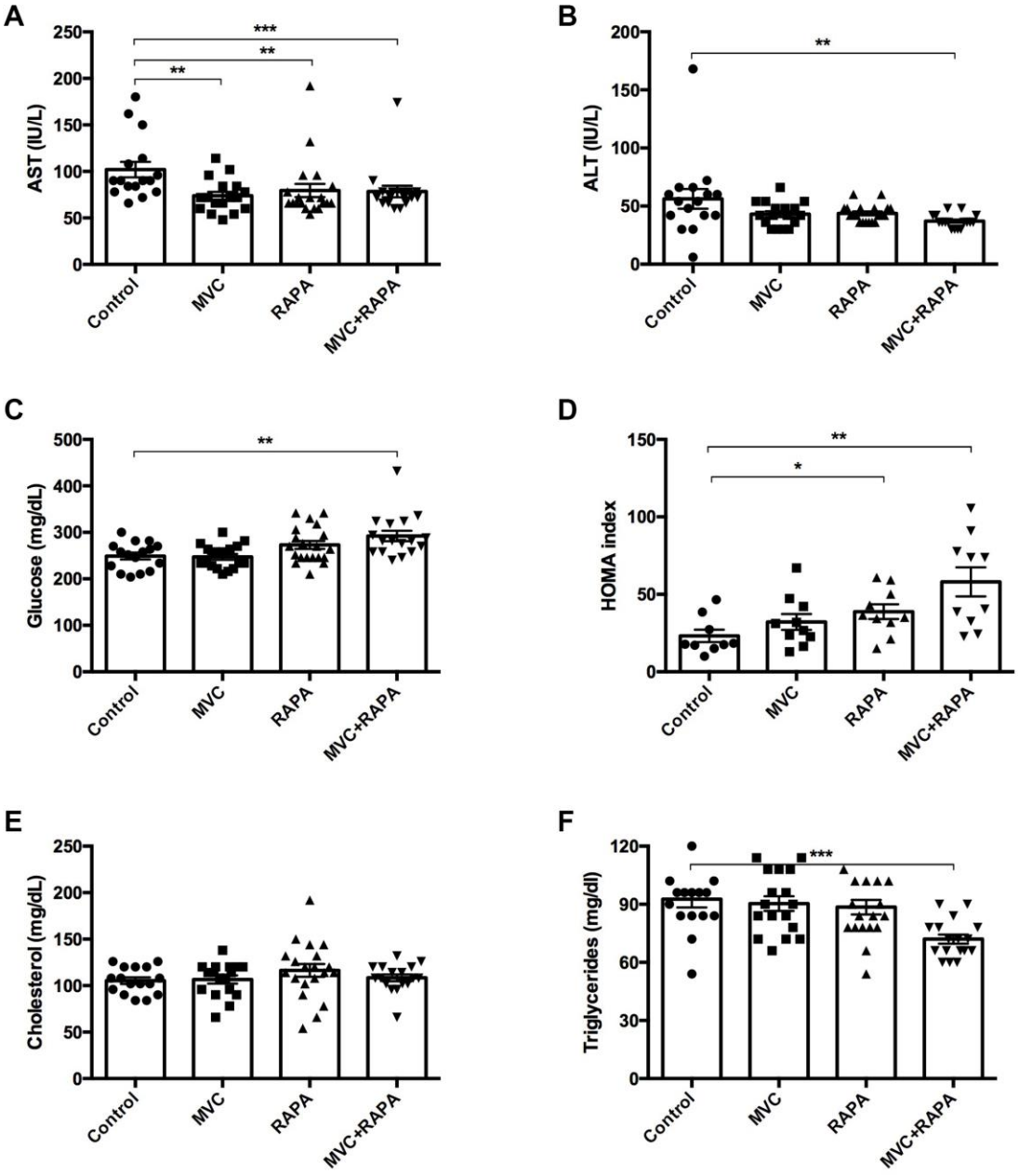

Figure 2. Biochemical and metabolic parameters: AST, ALT, glucose, HOMA index, cholesterol, triglycerides. (**A**) A significant decrease in AST levels was recorded in all the therapeutic groups. (**B**) There was a decrease in ALT levels in all the therapeutic groups but only statistically significant in the MVC+RAPA group. (**C**) Glucose levels were discreetly superior in all the therapeutic groups, but only significant in the MVC+RAPA group. (**D**) Compared to control group, HOMA index was significantly higher in RAPA and MVC+RAPA group. (**E**) No differences were observed in the groups after analyzing the cholesterol levels. (**F**). Compared to control group, significantly differences were only observed after comparing it to the MVC+RAPA group. Each bar represents the mean ± SEM. *p <0.05, **p <0.01 and ***p <0.001 with respect to control. ALT, alanine aminotransferase. AST, aspartate aminotransferase. MVC, maraviroc. RAPA, rapamycin. MVC+RAPA, maraviroc plus rapamycin.

MVC group showed a statistical reduction in myostatin after analyzing its expression in muscle; RAPA (p=0.001) and MVC-RAPA (p<0.0001). Similar findings were observed after analyzing serum samples; MVC (p<0.01), RAPA (p=0.01), and MVC-RAPA group (p=0.002). The levels of serum CK levels, a sensitive marker of muscle injury, were significantly lower in the MVC (p<0.002) and RAPA (p<0.01) groups. Nonetheless, the four groups had similar weights at the end of the experiment, and no significant differences were observed. Finally, contrary to expectations, muscle TC levels were significantly higher in the RAPA group (p=0.012), but no differences were observed after analyzing muscle TGD levels (Figure 3).

Skeletal muscle signaling showed differences only after analyzing caspase-3

IRS (1 and 2) showed no differences, although MVC-RAPA showed a tendency towards a lower level of IRS-2 (p=0.063). In the same way, SIRT (1, 3 and 6) showed no differences. Meanwhile, caspase-3, an inducer of apoptosis, was significantly lower in the MVC (p=0.011) and RAPA groups (p<0.05), showing also a clear tendency in the MVC-RAPA group (p=0.063). Finally, NFKB (1 and 2) showed no differences (Figure 4).

Effects on cytokines or chemokines

In this study, no differences were observed after analyzing muscle IL-1β. However, IL-6 levels were significantly lower in the MVC-RAPA group (p=0.028) and showed a tendency in the MVC group (p=0.089). Likewise, in muscle samples, IL-18 levels, another pro-inflammatory cytokine, were significantly lower in the MVC groups (p=0.014). No differences were observed after analyzing TNF-α. In the same way, no differences were observed after analyzing serum IL-1β, IL-6, or TNF-α (data not shown). In reference to chemokines, no differences in muscle CCR5 expression were observed after analyzing the different groups although there was a clear tendency in the RAPA group (p=0.054). Similarly, muscle CCL5 expression was significantly lower in the MVC group (p=0.035) and showed a clear tendency in the RAPA and MVC-RAPA groups (p=0.063 and p=0.052, respectively) (Figure 5).

WB analysis showed

That mice treated with MVC showed a significant decrease in caspase-3 (p <0.01) and IRS1 (p <0.05). In addition, the RAPA group showed a decrease in p-NFKB (p <0.01) and SIRT3 (p <0.0001) but an increase in total NFKB (p <0.01) and IRS2 (p <0.01). The MVC-RAPA group showed a significant increase in the p-AKT (p <0.001), total NFKB (p <0.01), p-mTOR (p <0.0001), SIRT1 (p <0.01) and IRS2 (p< 0.01), but a decrease in SIRT3 (Figure 6). It is worth noting that the decrease in caspase-3 protein upon MVC treatment was also observed at the mRNA level (Figure 4), while other effects may be different at the protein and mRNA levels due to differences in translation efficiency and/or protein stability. Interestingly, MVC-RAPA group showed a synergistic effect on p-AKT and SIRT1 protein levels, which are increased only by their combined treatment.

Histological assessment of skeletal muscle

H&E and Masson's trichrome staining showed no differences in any of the four groups (data not shown).

No differences were observed after analyzing frailty parameters

At the end of the experiment, no differences were observed after analyzing the frailty index score, time on rotarod, grip strength or endurance. However there was a favorable trend in grip strength in the RAPA (p=0.095) and MVC-RAPA (p=0.091) groups. In addition, endurance also showed a tendency towards improvement in the RAPA group (p=0.097) (Figure 7).

DISCUSSION

To properly manage frailty it is necessary to improve the knowledge of this syndrome. To reduce frailty, exercise programs and nutritional supplementation have been proposed as strategies to prevent and treat frailty and sarcopenia [34]. Now, in this animal model, we show interesting data about the possibility of adding a therapeutic strategy such as MVC.

First, we have shown the beneficial effects of MVC and RAPA on myostatin, a negative regulator of muscle mass [35] that has been implicated in wasting conditions such as sarcopenia and cachexia [36]. In addition to the effects of myostatin on muscle mass, muscle myostatin deficiency has beneficial effects on metabolism, adiposity and insulin sensitivity [37]. Although previous studies have shown that muscle myostatin was not affected by RAPA administration [38], we have observed a decrease in its levels. To our knowledge, this effect has not been described previously for MVC.

Another issue is the controversial relationship between serum levels of myostatin and frailty. Regarding older adults, some authors [39, 40] observed a direct correlation between serum myostatin levels and skeletal muscle mass, while others [41] found that muscle mass

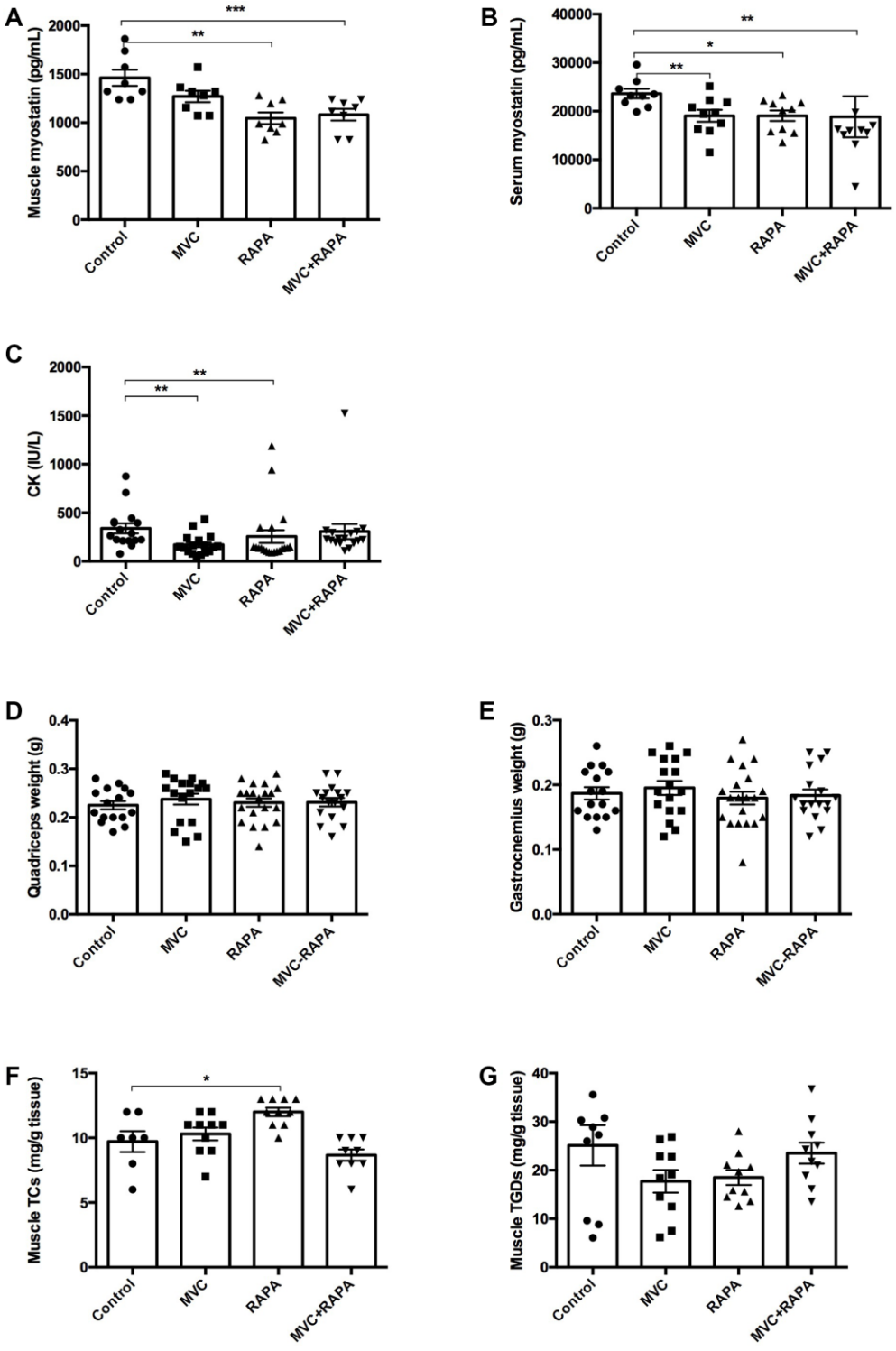

Figure 3. Biochemical and parameters related to muscle: Muscle and serum myostatin, CK, quadriceps and gastrocnemius weight, muscle cholesterol and triglyceride content. (**A**) A significant decrease in muscle myostatin levels was recorded in RAPA and MVC+RAPA groups. (**B**) There was a significative decrease in serum myostatin levels in all the therapeutic groups. (**C**) CK was significantly reduced in MVC and RAPA groups. No differences were observed after comparing the different groups for (**D**) quadriceps or (**E**) gastrocnemius weight. (**F**) Muscle cholesterol content was significantly higher in the RAPA groups. (**G**) Although muscle triglyceride content was lower in all the therapeutics groups, no differences were observed. Each bar represents the mean ± SEM. *p <0.05, **p <0.01 and ***p <0.001 with respect to control. CT, cholesterol total. CK, creatinkinase. MVC, maraviroc. MVC+RAPA, maraviroc plus rapamycin. RAPA, rapamycin. TGD, triglyceride.

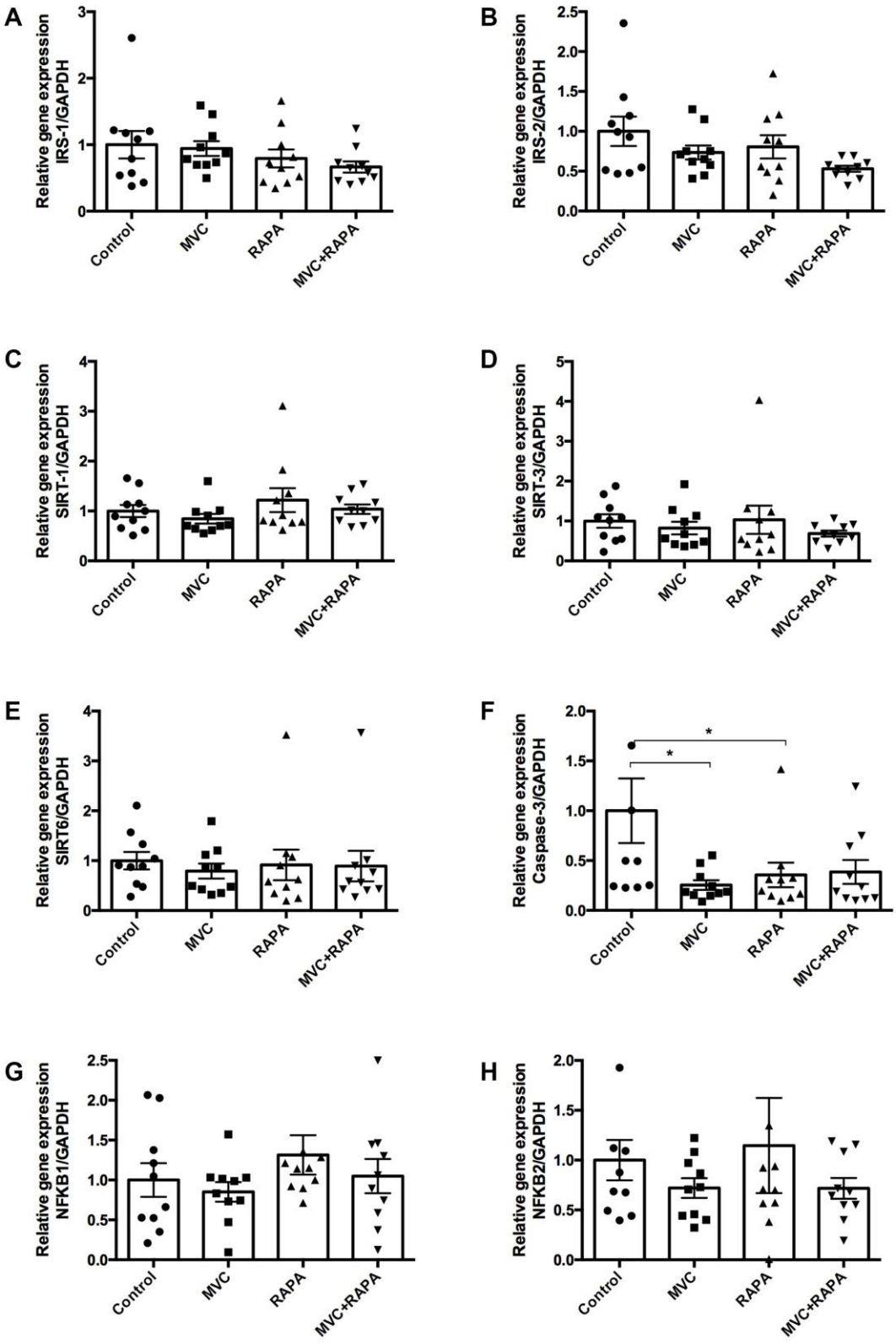

Figure 4. Muscle expression of insulin receptor substrate (1, 2), sirtuin (1-3), caspase-3, and nuclear factor KB at the RNA level. No differences were observed after analyzing (**A**) IRS-1, (**B**) IRS-2, (**C**) SIRT-1, (**D**) SIRT-3, or (**E**) SIRT-6. (**F**) Although caspase-3 was lower in all the therapeutics groups it was only statistically significant in MVC and RAPA groups. No differences were observed after analyzing (**G**) NFKB-1 and (**H**) NFKB-2. Each bar represents the mean ± SEM. *p <0.05 with respect to control. IRS, insulin receptor substrate. MVC, maraviroc. MVC+RAPA, maraviroc plus rapamycin. NFKB, nuclear factor KB. RAPA, rapamycin. SIRT, sirtuin.

was inversely correlated with serum myostatin levels. The differences in the results are mainly related to the assessment tool used to characterize frailty. In our project, we observed a decrease in the serum and muscular levels of myostatin in all therapeutic groups. As far as we know, we have not found studies that correlate serum and muscle levels of myostatin; therefore this study could also provide more clarity to the existing controversy.

Second, levels of serum CK, a sensitive marker of muscle injury [42], were significantly lower in the MVC and RAPA groups. In line with this observation and as far as we know, in the literature, there is a report

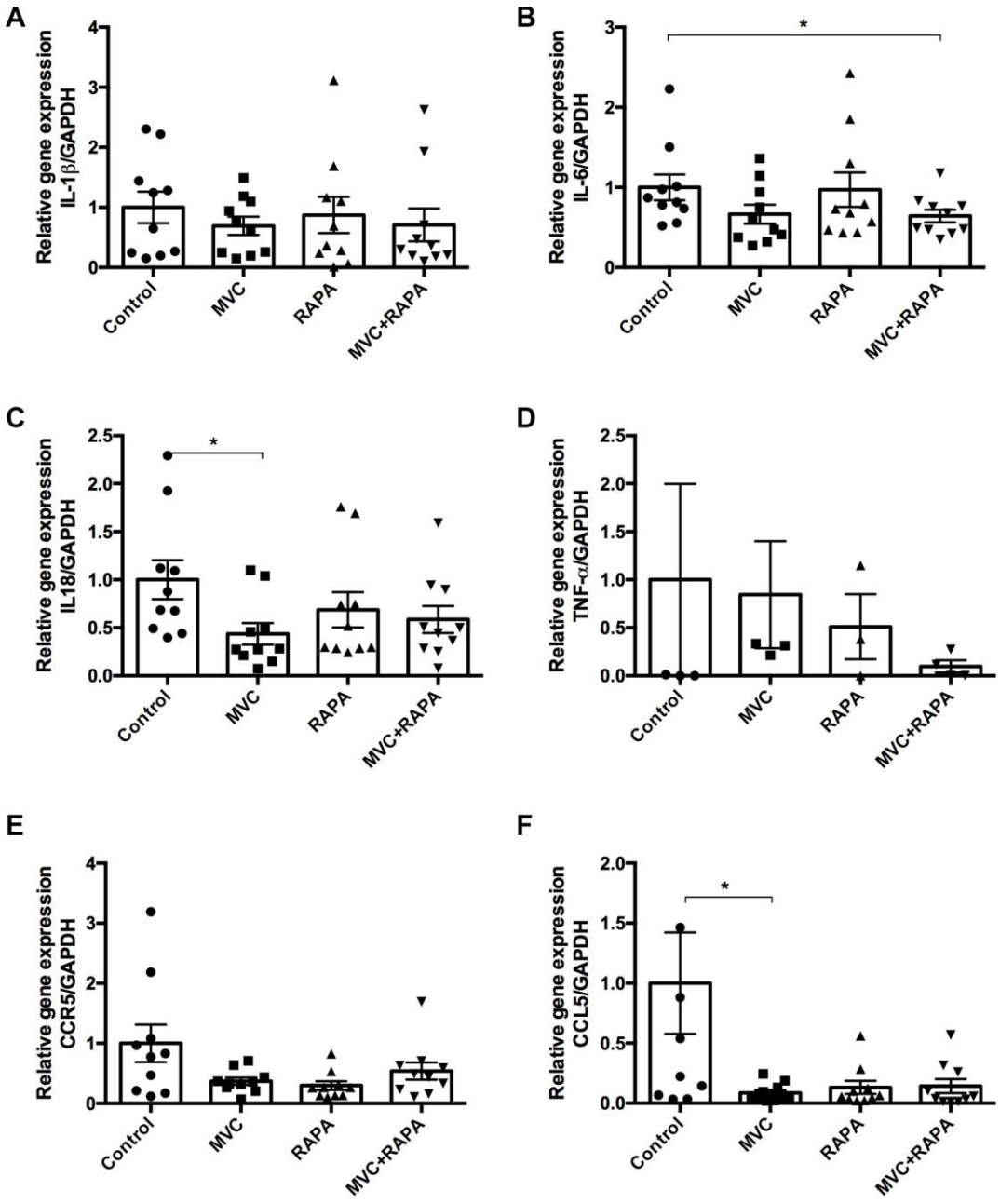

Figure 5. Muscle expression of IL-1β, IL6, IL-18, TNF-α, CCR5 and CCL5 at the RNA level. (**A**) No differences were observed after analyzing IL-1β. (**B**) IL-6 expression was significantly lower in the MVC+RAPA group. (**C**) Although IL-18 expression was lower in all the therapeutic groups, it was only statistically significant in the MVC group. (**D**) Although TNF-α and (**E**) CCR5 expression were lower in all the therapeutic groups, none of them was statistically significant. (**F**) CCL5 expression was significantly lower in the MVC group and showed a clear tendency to statistical significance in the RAPA and MVC-RAPA group. Each bar represents the mean ± SEM. *p <0.05 with respect to control. IL, interleukin. MVC, maraviroc. MVC+RAPA, maraviroc plus rapamycin. RAPA, rapamycin. TNF-α, tumor necrosis factor-alpha.

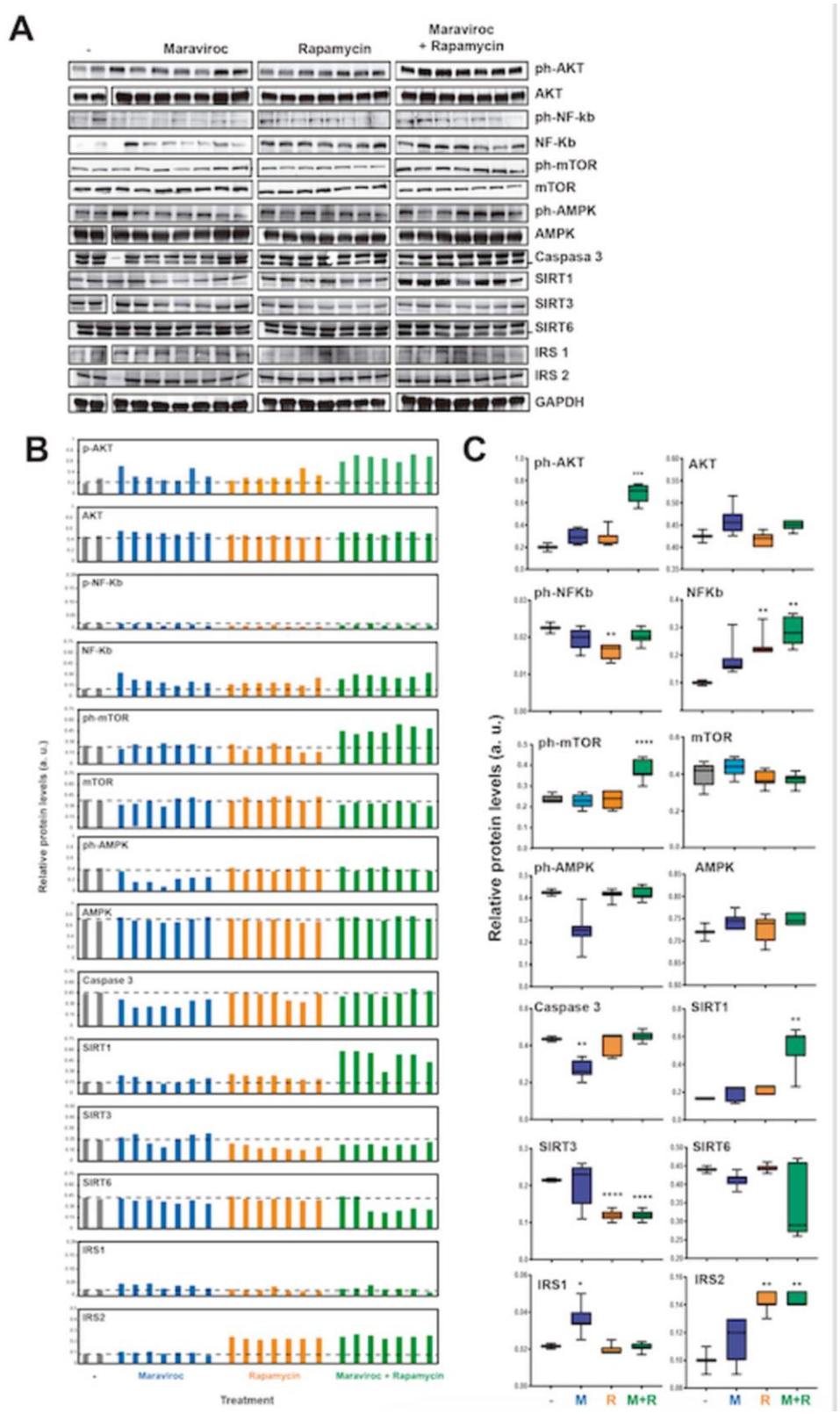

Figure 6. Analyses of the molecular pathways involved in the mechanism of action of RAPA and MVC (**A**) Western blot analysis of the protein levels of AKT (phosphorylated and total), NF-kb (phosphorylated and total), mTOR, AMPK (phosphorylated and total), Caspase 3, SIRT1, SIRT3, SIRT6, IRS1, IRS2 and GAPDH as endogenous control, in mice treated or not with maraviroc (MVC group), Rapamycin (RAPA group) or combination of both (MVC-RAPA group). (**B**) Relative quantification of the protein levels in (**A**) relative to GAPDH control. (**C**) Box plots showing the average protein levels from (**B**). Data were analyzed using Student t test´s. *, $P < 0.05$; **, $P < 0.01$; ***, $P < 0.001$; ****, $P < 0.0001$.

of and elderly HIV-infected patient with disabling inflammatory myopathy who had a reduction of his myositis after starting MVC [43], which would suggest its beneficial effect at the muscular level. No references have been found about the potential beneficial effect of RAPA on serum CK levels.

Third, AST levels, and in some way ALT levels, were lower in all the therapeutic groups. No references have been found about the potential beneficial effect of RAPA on AST levels. Although AST and ALT are important hepatotoxic biomarkers, they are also a biochemical marker of muscular damage [42]. Therefore, in chronic muscle injury, AST and ALT are both increased. In a study performed in the general population, sarcopenia was a risk factor for elevated aminotransferase in men independent of body mass index, dietary habits, and physical activity [44].

Fourth, caspases are crucial mediators of apoptosis. In this study, nearly all the therapeutic groups, in particular the MVC group, showed lower levels of caspase-3. This decrease in caspase-3 expression upon MVC treatment was also observed at the protein level. Previous studies showed an upregulation of caspase activity and apoptosis in old rats [45] and elderly persons [46]. Indeed, because apoptotic death is observed in multiple myopathies, it has been suggested that its inhibition could be a potential therapeutic strategy in the treatment of these disorders [47]. It will be necessary to evaluate the clinical potential of our observations.

All these observations support the idea that MVC and RAPA, both of which are CCR5 antagonists, could protect against muscle damage. In this sense, in an animal model of progressive muscle weakness, such as Duchenne muscular dystrophy, Liang et al. [48] observed that cenicriviroc (CVC), a dual chemokine receptor (CCR2/CCR5) antagonist, could slow disease progression. In their experiment they observed an important reduction in total infiltrating macrophages but not changes in muscle fiber size or fibrosis. In addition, the authors also observed an increase in the maximal isometric force production with CVC therapy [48].

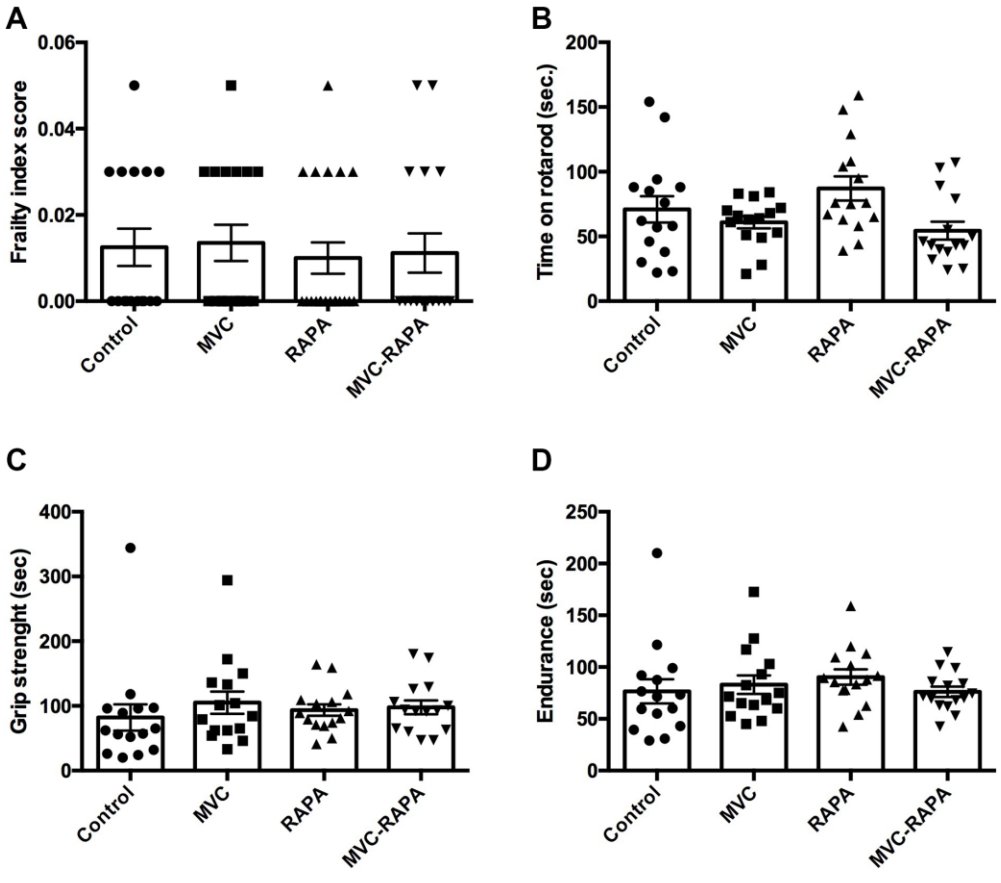

Figure 7. Frailty parameters: frailty index score, time on rotarod, grip strength, and endurance. No differences were observed after analyzing any of the frailty parameter for (**A**) frailty index score, (**B**) time on rotarod, (**C**) grip strength, and (**D**) endurance. Each bar represents the mean ± SEM. MVC, maraviroc. MVC+RAPA, maraviroc plus rapamycin. RAPA, rapamycin.

Previous studies have shown the ability of MVC to ameliorate the increased adipose tissue macrophage recruitment induced by a high-fat-diet mouse model of obesity [49]. Something similar was observed employing a murine model of genetic dyslipidaemia. In this case, MVC was able to inhibited atherosclerotic progression, among others, by reducing macrophage infiltration [50].

Against what we would have expected, in this animal model, we did not observe changes in the main cytokine levels. Therefore, it is possible that the potential protective effect of MVC and RAPA in this model of frailty does not depend on a pro-inflammatory or anti-inflammatory route. This is an aspect of interest because, at least in humans, the CCR5 RNA expression of skeletal muscle is very low (approximately 4 and 30 times lower than corresponding levels in the liver and peripheral blood lymphocytes, respectively) [51]. Indeed, despite the fact that both MVC and RAPA have anti-CCR5 effects, each of them also has a different impact on most of the tests analyzed, with some notable exceptions (i.e. AST, myostatin).

Finally, it is known that RAPA administration decreases CCR5 mRNA expression both *in vitro* [15] and *in vivo* (macaques) [16]. In addition, RAPA induced a synergistic enhancement of the CCR5 antagonists effects of vicroviroc [19] and aplaviroc [20] against HIV. To our knowledge, no studies have been performed on the synergistic effect of RAPA plus MVC. In this animal model, we did not observe a synergistic, additive or antagonistic effect on the level of CCR5 expression in the MVC-RAPA group. However, a synergistic increase in p-AKT, p-mTOR and SIRT1 protein levels upon MVC-RAPA treatment was observed, suggesting that they could have a protective effect.

This study could have some limitations. First, life extension by RAPA is more prominent at higher doses [14] than the dose we have employed. However, our objective was not to improve survival. Indeed, there is a concern about potential side effects (i.e., glucose intolerance or insulin resistance) [52, 53] that may limit MVC-RAPA use as an anti-aging drug. Because it is known that deficiency of CCR5 impairs systemic glucose tolerance [54], the double impact on CCR5 (MVC plus RAPA) may be the reason for the highest increases in the HOMA index.

In summary, our data could support that MVC and RAPA have a protective role in some factors involved in the development of frailty. These data could justify a randomized, controlled trial to determine their beneficial effects on patients with frailty.

MATERIALS AND METHODS

Animals and animal models

A total of 80 male homozygous IL-10 deficient mice (B6.129P2-IL10^{tm1Cgn}/J) were purchased from Jackson Laboratory (Bar Harbor, ME, USA). All animals were housed in pathogen-free barrier conditions and had free access to food and drinking water during the study. When the animals were approximately 6 weeks old, they were randomly assigned (n = 20) to one of 4 groups and fed for 24 weeks: i) the IL-10KO group (IL-10KO) received a standard rodent diet and tap water; ii) the preventive MVC group received the same diet as the IL-10KO group and received MVC (Pfizer, New York, NY) in their drinking water (300 mg/L) [21–23]; iii) the preventive RAPA group [24] received the same diet as the IL-10KO group and received RAPA in their drinking water (1.5 mg/kg/day) [25]; and iv) the preventive MVC plus RAPA group (MVC-RAPA) received the same diet as the IL-10KO group and received MVC plus RAPA in their drinking water at the same concentration as the MVC or RAPA group.

The mice were observed daily, and all the observations were recorded. In addition, the animals were weighed once a week. All the animals were sacrificed at week 24. At that time, blood samples were collected under anaesthesia after a 4-hour fasting period.

Blood sampling and analysis

Plasma levels of aspartate aminotransferase (AST), alanine aminotransferase (ALT), glucose, triglycerides (TGD), cholesterol (TC) and creatine kinase (CK) were measured using an automatic biochemical analyzer (Cobas C711, Roche, Madrid, Spain). Insulin resistance and insulin sensitivity were determined by using the homeostasis model assessment of insulin resistance (HOMA-IR) [26]. Glucose tolerance test was measured 14 days before sacrificing the animals [27]. Serum myostatin levels were measured by using an ELISA kit (R&D Systems).

Muscle preparation

Skeletal muscle tissues (quadriceps and gastrocnemius) were excised, weighed and frozen in liquid nitrogen and stored at -80 °C until processing.

To quantify muscle TGD and TC content, 150 mg of muscle tissue was homogenized in 1.5 mL of buffer (150 mM NaCl, 0.1% Triton X-100 and 10 mM Tris pH

8) at 50ºC using an Ultraturrax (IKA-Weke, Staufen, Germany) homogenizer. After the centrifugation of the homogenate at 12,000 g for 10 minutes, an autoanalyser was used to measure the TGD and TC levels in the obtained supernatant. Muscle myostatin levels were measured by using an ELISA kit (R&D Systems).

Gene expression quantification

Total RNA was extracted and purified from muscle samples using an RNA RNeasy Mini Kit (Qiagen, Valencia, CA), and was treated with DNase I (Qiagen) following the manufacturer's instructions. cDNA was synthesized by reverse transcription of 1 µg of total RNA using the SuperScript III First-Strand Synthesis kit (Invitrogen) in a total volume of 30 µl according to the manufacturer's instructions, followed by amplification using SybrGreen (Takara Bio Inc., Shiga, Japan) PCR.rt using specific primers (Supplementary Table 1).

Amplification and detection of specific products were performed using the ABI PRISM 7300 (Applied Biosystems, Foster City, CA, USA). All reactions were run in duplicate for each studied sample. The relative expression of the biomarkers analyzed was calculated according to the manufacturers' instructions. All the results were divided by their corresponding housekeeping gene value.

Sandwich enzyme linked immunosorbent assay (ELISA)

TNF-α, IL-1β, IL-6 and myostatin levels were quantified in serum samples (Supplementary Table 2). The serum was separated from the cells after clot formation by centrifugation. For each assay performed, a minimum of 2 wells must be used as blanks; therefore, primary antibodies were not applied to those wells. The ELISA plate (Nunc Maxisorp) was coated with 100 µl/well of capture antibody in 1X Coating Buffer. The plate was sealed and incubated overnight at 4°C. All wells were aspirated and washed 5 times with 300 µl/well of Wash Buffer.

Afterwards, the wells were blocked with 200 µl/well of 1X ELISA Diluent and incubated at room temperature for 1 hour. To activate the latent antibody to its immunoreactive form, the samples (but not the standards) were acidified and then neutralized. The mouse serum was diluted 1:8 in PBS. Per 100 µl of sample, 20 µl of 1N HCl was added and incubated for 10 minutes at room temperature and then neutralized with 20 µl of 1N NaOH. Using 1X ELISA Diluent, 2-fold serial dilutions of the top standards were performed to make a standard curve. A volume of 100 µl/well of the standard dilutions was added to the appropriate wells. In the same way, 100 µl/well of the acid-activated samples was added to the appropriate wells. The plate was sealed and incubated at room temperature for 2 hours. After this time, the wells were aspirated and washed 4 times with 300 µl/well of Wash Buffer. Then, 100 µl of detection antibody diluted in 1X ELISA Diluent was added to each well and incubated at room temperature for 1 hour. All wells were aspirated and washed 5 times. A volume of 100 µl/well of Avidin-HRP diluted in 1X ELISA Diluent was added and the plate was incubated at room temperature for 30 minutes. The wells were aspirated and washed 7 times. A volume of 100 µl of 1X TMB Solution was added to each well and the plate was incubated at room temperature for 15 minutes. Afterward, 50 µl of Stop Solution was added to each well. The plate was read at 450 nm and 570 nm.

Western blot analysis

Muscle samples were lysed using a homogenizer and treated with RIPA lysis buffer (Sigma Aldrich, St. Louis, MO). The cell lysate was centrifuged at 10,000 g for 10 minutes at 4ºC. The concentration of total protein in each sample was determined by the Bradford method.

5'-Adenosine monophosphate-activated protein kinase (AMPK), phosphorylated

AMPK (pAMPK), protein kinase-B (Akt), phosphorylated AKT, nuclear factor-kB (NFKB), phosphorylated NFKB (pNFKB), mTOR, phosphorylated mTOR, sirtuin (SIRT) (1, 3, and 6), insulin receptor substrates (IRS) (1 and 2), and caspase-3 were evaluated by Western blotting (WB). GAPDH was used as a control (Supplementary Table 3).

Samples (30 µg per well) were subjected to polyacrylamide gel electrophoresis (SDS–PAGE). Subsequently, the proteins were transferred to a nitrocellulose membrane that was incubated with a specific antibody against the proteins of interest. Proteins were detected by colorimetry using a secondary antibody bound to the peroxidase enzyme (Anti-rabbit IgG, Cell Signaling, Danvers, MA) and incubation with the corresponding substrate. After high-resolution scanning, the concentration of each protein was evaluated by densitometry using ImageJ software. The density values for each of the test samples were normalized based on the values of GAPDH, which was used as a loading control.

Muscle fiber staining

Following fixation, skeletal muscle tissues (quadriceps and gastrocnemius) were dehydrated and paraffin

embedded. Tissue sections (3 μm-thick) were rehydrated and stained according to standard protocols with hematoxylin and eosin (H&E) and Masson's trichrome staining, which stains muscle fibers red, nuclei black, and collagen blue. Muscle fiber size was measured using ImageJ software.

Survival study

Animals were inspected daily for health issues, and deaths were recorded for each animal. Mice were euthanized for humane reasons if so severely moribund that they were considered by an experienced technician, unlikely to survive for more than an additional 48 hours. Moribund animals were euthanized by CO_2 asphyxiation and recorded. Every animal found dead or euthanized was necropsied. Criteria for euthanasia were considered by an experienced technician, according to the AAALAC guidelines. For the longevity study, only cases where the condition of the animal was considered incompatible with continued survival are represented as deaths in the curves. Animals removed at sacrifice or euthanized due to reasons not related to incompatible survival were considered censored deaths.

Frailty index assessment

A frailty index (FI) score was calculated for each mouse using the 31-item FI [28]. The sum of the scores for 31 items was divided by 31 to give the FI. The validity of this scale was correlated with human FI and had a good agreement [28]. The temperature and weight scores were calculated based on the number of standard deviations of the tested mouse compared with the reference values from sex-matched adult animals.

Functional assessment

The inverted-cling grip test was used for evaluating the grip strength of limbs and the endurance of muscles in the mice [29]. This procedure was performed as proposed by Liu et al. [30]. The walking speed was evaluated using the rotarod test (RotaRod R/S; LSi Letica, Cornella, Spain). The rotarod test is widely used for determining overall motor function in mice [29]. This procedure was performed as proposed by Liu et al. [30]. Finally, both the grip test and the rotarod test were used to assess overall endurance [29]. The equation employed was [(Endurance score (seconds) = (Time of grip test + Time of rotarod test)/2)].

Statistics

Data are presented in the figures as the mean ± SEM (standard error of the mean). Body weight data were analyzed with analysis of variance followed by the Dunnet post-hoc test. For all other data, the Kruskal–Wallis test was used followed by the Mann–Whitney U-test. Correlation between variables was determined using the Spearman rank-sum test. Survival analysis was performed using Kaplan–Meier survival analysis. All data were analyzed with GraphPad Prism 6 software and were considered statistically significant when $p<0.05$.

Ethics statement

All procedures were carried out in accordance with the European Communities Council Directive (86/609/CEE) on animal experiments and with approval from the ethical committee on animal welfare of our institution (Comité Etico de Experimentación Animal del Centro de Investigación Biomédica de La Rioja, CEEA-CIBIR).

AUTHOR CONTRIBUTIONS

Conceived and designed the project: JRB, LP, LR, AC. Performed the experiments: LP, LR, SMG, SRM, EMVS. Analyzed the data: JRB, JAO, LP, LR, SMG, AC. Wrote the paper: JRB.

ACKNOWLEDGMENTS

Maraviroc and Rapamycin were a generous gift from Pfizer.

CONFLICTS OF INTEREST

Dr. L Pérez-Martínez has received compensation for lectures from Abbvie, Bristol-Myers Squibb, Gilead Sciences, and Janssen. Dr. JA Oteo has carried out consulting work for Abbvie, Bristol-Myers Squibb, Gilead Sciences, Janssen, Merck, and ViiV Healthcare; has received compensation for lectures from Abbvie, Bristol-Myers Squibb, Gilead Sciences, Janssen, Merck, and ViiV Healthcare, as well as grants and payments for the development of educational presentations for Gilead Sciences, Bristol-Myers Squibb and ViiV Healthcare. Dr. JR Blanco has carried out consulting work for Abbvie, Bristol-Myers Squibb, Gilead Sciences, Janssen, Merck, and ViiV Healthcare; has received compensation for lectures from Abbvie, Bristol-Myers Squibb, Gilead Sciences, Janssen, Merck, and ViiV Healthcare, as well as grants and payments for the development of educational presentations for Gilead Sciences, Bristol-Myers Squibb and ViiV Healthcare. The rest of the authors declare no conflicts of interest.

FUNDING

This study was partially supported by the Instituto de Salud Carlos III (ISCIII), M. Economía y Competitividad of Spain [Project Fondo de

Investigaciones Sanitarias PI16/00127 (Acción Estratégica en Salud 2013-2016)]. Co-funded by European Regional Development Fund (FEDER) "A way to make Europe", by the Fondos FEDER, Convocatoria de ayudas a grupos de investigación para el desarrollo de proyectos de investigación, desarrollo tecnológico e innovación en el sector biomédico (Convocatoria FEDER-La Rioja; FRSABC007), and RTI2018-097455-B-I00 (MCIU/AEI/FEDER, UE); CIBER de Cáncer (CB16/12/00275). The funder had no role in study design, data collection and analysis, decision to publish, or preparation of the manuscript.

REFERENCES

1. United Nations Department of Economic and Social Affairs (DESA)/Population Division. World Population Prospects. 2019. Available at: https://population.un.org/wpp/Download/Standard/Population/

2. Rodríguez Mañas L. Determinants of Frailty and Longevity: Are They the Same Ones? Nestle Nutr Inst Workshop Ser. 2015; 83:29–39. https://doi.org/10.1159/000382057 PMID:26485702

3. Rockwood K, Stadnyk K, MacKnight C, McDowell I, Hébert R, Hogan DB. A brief clinical instrument to classify frailty in elderly people. Lancet. 1999; 353:205–06. https://doi.org/10.1016/S0140-6736(98)04402-X PMID:9923878

4. Fried LP, Tangen CM, Walston J, Newman AB, Hirsch C, Gottdiener J, Seeman T, Tracy R, Kop WJ, Burke G, McBurnie MA, and Cardiovascular Health Study Collaborative Research Group. Frailty in older adults: evidence for a phenotype. J Gerontol A Biol Sci Med Sci. 2001; 56:M146–56. https://doi.org/10.1093/gerona/56.3.M146 PMID:11253156

5. Cruz-Jentoft AJ, Bahat G, Bauer J, Boirie Y, Bruyère O, Cederholm T, Cooper C, Landi F, Rolland Y, Sayer AA, Schneider SM, Sieber CC, Topinkova E, et al, and Writing Group for the European Working Group on Sarcopenia in Older People 2 (EWGSOP2), and the Extended Group for EWGSOP2. Sarcopenia: revised European consensus on definition and diagnosis. Age Ageing. 2019; 48:16–31. https://doi.org/10.1093/ageing/afy169 PMID:30312372

6. Howlett SE. Assessment of Frailty in Animal Models. Interdiscip Top Gerontol Geriatr. 2015; 41:15–25. https://doi.org/10.1159/000381131 PMID:26301976

7. Walston J, Fedarko N, Yang H, Leng S, Beamer B, Espinoza S, Lipton A, Zheng H, Becker K. The physical and biological characterization of a frail mouse model. J Gerontol A Biol Sci Med Sci. 2008; 63:391–98. https://doi.org/10.1093/gerona/63.4.391 PMID:18426963

8. von Zglinicki T, Varela Nieto I, Brites D, Karagianni N, Ortolano S, Georgopoulos S, Cardoso AL, Novella S, Lepperdinger G, Trendelenburg AU, van Os R. Frailty in mouse ageing: A conceptual approach. Mech Ageing Dev. 2016; 160:34–40. https://doi.org/10.1016/j.mad.2016.07.004 PMID:27443148

9. Mannick JB, Del Giudice G, Lattanzi M, Valiante NM, Praestgaard J, Huang B, Lonetto MA, Maecker HT, Kovarik J, Carson S, Glass DJ, Klickstein LB. mTOR inhibition improves immune function in the elderly. Sci Transl Med. 2014; 6:268ra179. https://doi.org/10.1126/scitranslmed.3009892 PMID:25540326

10. Li J, Kim SG, Blenis J. Rapamycin: one drug, many effects. Cell Metab. 2014; 19:373–79. https://doi.org/10.1016/j.cmet.2014.01.001 PMID:24508508

11. Harrison DE, Strong R, Sharp ZD, Nelson JF, Astle CM, Flurkey K, Nadon NL, Wilkinson JE, Frenkel K, Carter CS, Pahor M, Javors MA, Fernandez E, Miller RA. Rapamycin fed late in life extends lifespan in genetically heterogeneous mice. Nature. 2009; 460:392–95. https://doi.org/10.1038/nature08221 PMID:19587680

12. Wilkinson JE, Burmeister L, Brooks SV, Chan CC, Friedline S, Harrison DE, Hejtmancik JF, Nadon N, Strong R, Wood LK, Woodward MA, Miller RA. Rapamycin slows aging in mice. Aging Cell. 2012; 11:675–82. https://doi.org/10.1111/j.1474-9726.2012.00832.x PMID:22587563

13. Miller RA, Harrison DE, Astle CM, Baur JA, Boyd AR, de Cabo R, Fernandez E, Flurkey K, Javors MA, Nelson JF, Orihuela CJ, Pletcher S, Sharp ZD, et al. Rapamycin, but not resveratrol or simvastatin, extends life span of genetically heterogeneous mice. J Gerontol A Biol Sci Med Sci. 2011; 66:191–201. https://doi.org/10.1093/gerona/glq178 PMID:20974732

14. Miller RA, Harrison DE, Astle CM, Fernandez E, Flurkey K, Han M, Javors MA, Li X, Nadon NL, Nelson JF, Pletcher S, Salmon AB, Sharp ZD, et al. Rapamycin-mediated lifespan increase in mice is dose and sex dependent and metabolically distinct from dietary restriction. Aging Cell. 2014; 13:468–77. https://doi.org/10.1111/acel.12194 PMID:24341993

15. Heredia A, Amoroso A, Davis C, Le N, Reardon E, Dominique JK, Klingebiel E, Gallo RC, Redfield RR. Rapamycin causes down-regulation of CCR5 and accumulation of anti-HIV beta-chemokines: an approach to suppress R5 strains of HIV-1. Proc Natl Acad Sci USA. 2003; 100:10411–16. https://doi.org/10.1073/pnas.1834278100 PMID:12915736

16. Gilliam BL, Heredia A, Devico A, Le N, Bamba D, Bryant JL, Pauza CD, Redfield RR. Rapamycin reduces CCR5 mRNA levels in macaques: potential applications in HIV-1 prevention and treatment. AIDS. 2007; 21:2108–10. https://doi.org/10.1097/QAD.0b013e3282f02a4f PMID:17885304

17. De Fanis U, Wang GC, Fedarko NS, Walston JD, Casolaro V, Leng SX. T-lymphocytes expressing CC chemokine receptor-5 are increased in frail older adults. J Am Geriatr Soc. 2008; 56:904–08. https://doi.org/10.1111/j.1532-5415.2008.01673.x PMID:18384587

18. Gilliam BL, Riedel DJ, Redfield RR. Clinical use of CCR5 inhibitors in HIV and beyond. J Transl Med. 2011 (Suppl 1); 9:S9. https://doi.org/10.1186/1479-5876-9-S1-S9 PMID:21284908

19. Heredia A, Latinovic O, Gallo RC, Melikyan G, Reitz M, Le N, Redfield RR. Reduction of CCR5 with low-dose rapamycin enhances the antiviral activity of vicriviroc against both sensitive and drug-resistant HIV-1. Proc Natl Acad Sci USA. 2008; 105:20476–81. https://doi.org/10.1073/pnas.0810843106 PMID:19075241

20. Latinovic O, Heredia A, Gallo RC, Reitz M, Le N, Redfield RR. Rapamycin enhances aplaviroc anti-HIV activity: implications for the clinical development of novel CCR5 antagonists. Antiviral Res. 2009; 83:86–89. https://doi.org/10.1016/j.antiviral.2009.02.199 PMID:19501260

21. Ochoa-Callejero L, Pérez-Martínez L, Rubio-Mediavilla S, Oteo JA, Martínez A, Blanco JR. Maraviroc, a CCR5 antagonist, prevents development of hepatocellular carcinoma in a mouse model. PLoS One. 2013; 8:e53992. https://doi.org/10.1371/journal.pone.0053992 PMID:23326556

22. Pérez-Martínez L, Pérez-Matute P, Aguilera-Lizarraga J, Rubio-Mediavilla S, Narro J, Recio E, Ochoa-Callejero L, Oteo JA, Blanco JR. Maraviroc, a CCR5 antagonist, ameliorates the development of hepatic steatosis in a mouse model of non-alcoholic fatty liver disease (NAFLD). J Antimicrob Chemother. 2014; 69:1903–10. https://doi.org/10.1093/jac/dku071 PMID:24651825

23. Neff CP, Ndolo T, Tandon A, Habu Y, Akkina R. Oral pre-exposure prophylaxis by anti-retrovirals raltegravir and maraviroc protects against HIV-1 vaginal transmission in a humanized mouse model. PLoS One. 2010; 5:e15257. https://doi.org/10.1371/journal.pone.0015257 PMID:21203568

24. Ridker PM, Cannon CP, Morrow D, Rifai N, Rose LM, McCabe CH, Pfeffer MA, Braunwald E, and Pravastatin or Atorvastatin Evaluation and Infection Therapy-Thrombolysis in Myocardial Infarction 22 (PROVE IT-TIMI 22) Investigators. C-reactive protein levels and outcomes after statin therapy. N Engl J Med. 2005; 352:20–28. https://doi.org/10.1056/NEJMoa042378 PMID:15635109

25. Komarova EA, Antoch MP, Novototskaya LR, Chernova OB, Paszkiewicz G, Leontieva OV, Blagosklonny MV, Gudkov AV. Rapamycin extends lifespan and delays tumorigenesis in heterozygous p53+/- mice. Aging (Albany NY). 2012; 4:709–14. https://doi.org/10.18632/aging.100498 PMID:23123616

26. Matthews DR, Hosker JP, Rudenski AS, Naylor BA, Treacher DF, Turner RC. Homeostasis model assessment: insulin resistance and beta-cell function from fasting plasma glucose and insulin concentrations in man. Diabetologia. 1985; 28:412–19. https://doi.org/10.1007/BF00280883 PMID:3899825

27. Pérez-Martínez L, Ochoa-Callejero L, Rubio-Mediavilla S, Narro J, Bernardo I, Oteo JA, Blanco JR. Maraviroc improves hepatic triglyceride content but not inflammation in a murine nonalcoholic fatty liver disease model induced by a chronic exposure to high-fat diet. Transl Res. 2018; 196:17–30. https://doi.org/10.1016/j.trsl.2018.01.004 PMID:29421523

28. Whitehead JC, Hildebrand BA, Sun M, Rockwood MR, Rose RA, Rockwood K, Howlett SE. A clinical frailty index in aging mice: comparisons with frailty index data in humans. J Gerontol A Biol Sci Med Sci. 2014; 69:621–32. https://doi.org/10.1093/gerona/glt136 PMID:24051346

29. Graber TG, Ferguson-Stegall L, Kim JH, Thompson LV. C57BL/6 neuromuscular healthspan scoring system. J Gerontol A Biol Sci Med Sci. 2013; 68:1326–36. https://doi.org/10.1093/gerona/glt032 PMID:23585418

30. Liu H, Graber TG, Ferguson-Stegall L, Thompson LV. Clinically relevant frailty index for mice. J Gerontol A

Biol Sci Med Sci. 2014; 69:1485–91.
https://doi.org/10.1093/gerona/glt188
PMID:24336799

31. Cobbold JF, Anstee QM, Thomas HC. Investigating mildly abnormal serum aminotransferase values. BMJ. 2010; 341:c4039.
https://doi.org/10.1136/bmj.c4039
PMID:20675393

32. Nathwani RA, Pais S, Reynolds TB, Kaplowitz N. Serum alanine aminotransferase in skeletal muscle diseases. Hepatology. 2005; 41:380–82.
https://doi.org/10.1002/hep.20548
PMID:15660433

33. Rodriguez J, Vernus B, Chelh I, Cassar-Malek I, Gabillard JC, Hadj Sassi A, Seiliez I, Picard B, Bonnieu A. Myostatin and the skeletal muscle atrophy and hypertrophy signaling pathways. Cell Mol Life Sci. 2014; 71:4361–71.
https://doi.org/10.1007/s00018-014-1689-x
PMID:25080109

34. Nascimento CM, Ingles M, Salvador-Pascual A, Cominetti MR, Gomez-Cabrera MC, Viña J. Sarcopenia, frailty and their prevention by exercise. Free Radic Biol Med. 2019; 132:42–49.
https://doi.org/10.1016/j.freeradbiomed.2018.08.035
PMID:30176345

35. McPherron AC, Lawler AM, Lee SJ. Regulation of skeletal muscle mass in mice by a new TGF-beta superfamily member. Nature. 1997; 387:83–90.
https://doi.org/10.1038/387083a0
PMID:9139826

36. Elkina Y, von Haehling S, Anker SD, Springer J. The role of myostatin in muscle wasting: an overview. J Cachexia Sarcopenia Muscle. 2011; 2:143–51.
https://doi.org/10.1007/s13539-011-0035-5
PMID:21966641

37. Consitt LA, Clark BC. The Vicious Cycle of Myostatin Signaling in Sarcopenic Obesity: Myostatin Role in Skeletal Muscle Growth, Insulin Signaling and Implications for Clinical Trials. J Frailty Aging. 2018; 7:21–27.
https://doi.org/10.14283/jfa.2017.33
PMID:29412438

38. Choi DH, Yang J, Kim YS. Rapamycin suppresses postnatal muscle hypertrophy induced by myostatin-inhibition accompanied by transcriptional suppression of the Akt/mTOR pathway. Biochem Biophys Rep. 2019; 17:182–90.
https://doi.org/10.1016/j.bbrep.2018.12.009
PMID:30805561

39. Arrieta H, Hervás G, Rezola-Pardo C, Ruiz-Litago F, Iturburu M, Yanguas JJ, Gil SM, Rodriguez-Larrad A, Irazusta J. Serum myostatin levels are higher in fitter, more active, and non-frail long-term nursing home residents and increase after a physical exercise intervention. Gerontology. 2019; 65:229–39.
https://doi.org/10.1159/000494137
PMID:30463070

40. Peng LN, Lee WJ, Liu LK, Lin MH, Chen LK. Healthy community-living older men differ from women in associations between myostatin levels and skeletal muscle mass. J Cachexia Sarcopenia Muscle. 2018; 9:635–42.
https://doi.org/10.1002/jcsm.12302
PMID:29654636

41. Yarasheski KE, Bhasin S, Sinha-Hikim I, Pak-Loduca J, Gonzalez-Cadavid NF. Serum myostatin-immunoreactive protein is increased in 60-92 year old women and men with muscle wasting. J Nutr Health Aging. 2002; 6:343–48.
PMID:12474026

42. Brancaccio P, Lippi G, Maffulli N. Biochemical markers of muscular damage. Clin Chem Lab Med. 2010; 48:757–67.
https://doi.org/10.1515/CCLM.2010.179
PMID:20518645

43. Capetti AF, Pocaterra D, Zucchi P, Carenzi L, Rizzardini G. Anti-inflammatory effect of maraviroc in an HIV-infected patient with concomitant myositis: a case report. J Int Assoc Physicians AIDS Care (Chic). 2010; 9:201–02.
https://doi.org/10.1177/1545109710372671
PMID:20798399

44. Yoo KD, Jun DW, Lee KN, Lee HL, Lee OY, Yoon BC, Choi HS. Sarcopenia is a risk factor for elevated aminotransferase in men independently of body mass index, dietary habits, and physical activity. Dig Liver Dis. 2015; 47:303–08.
https://doi.org/10.1016/j.dld.2014.12.014
PMID:25618554

45. Chung L, Ng YC. Age-related alterations in expression of apoptosis regulatory proteins and heat shock proteins in rat skeletal muscle. Biochim Biophys Acta. 2006; 1762:103–09.
https://doi.org/10.1016/j.bbadis.2005.08.003
PMID:16139996

46. Whitman SA, Wacker MJ, Richmond SR, Godard MP. Contributions of the ubiquitin-proteasome pathway and apoptosis to human skeletal muscle wasting with age. Pflugers Arch. 2005; 450:437–46.
https://doi.org/10.1007/s00424-005-1473-8
PMID:15952031

47. Sandri M, El Meslemani AH, Sandri C, Schjerling P, Vissing K, Andersen JL, Rossini K, Carraro U, Angelini C.

Caspase 3 expression correlates with skeletal muscle apoptosis in Duchenne and facioscapulo human muscular dystrophy. A potential target for pharmacological treatment? J Neuropathol Exp Neurol. 2001; 60:302–12.
https://doi.org/10.1093/jnen/60.3.302
PMID:11245214

48. Liang F, Giordano C, Shang D, Li Q, Petrof BJ. The dual CCR2/CCR5 chemokine receptor antagonist Cenicriviroc reduces macrophage infiltration and disease severity in Duchenne muscular dystrophy (Dmdmdx-4Cv) mice. PLoS One. 2018; 13:e0194421.
https://doi.org/10.1371/journal.pone.0194421
PMID:29561896

49. Pérez-Matute P, Pichel JG, Iñiguez M, Recio-Fernández E, Pérez-Martínez L, Torrens R, Blanco JR, Oteo JA. Maraviroc ameliorates the increased adipose tissue macrophage recruitment induced by a high-fat diet in a mouse model of obesity. Antivir Ther. 2017; 22:163–68.
https://doi.org/10.3851/IMP3099
PMID:27725337

50. Cipriani S, Francisci D, Mencarelli A, Renga B, Schiaroli E, D'Amore C, Baldelli F, Fiorucci S. Efficacy of the CCR5 antagonist maraviroc in reducing early, ritonavir-induced atherogenesis and advanced plaque progression in mice. Circulation. 2013; 127:2114–24.
https://doi.org/10.1161/CIRCULATIONAHA.113.001278
PMID:23633271

51. The human protein atlas. Available at:
https://www.proteinatlas.org/ENSG00000160791-CCR5/tissue

52. Deblon N, Bourgoin L, Veyrat-Durebex C, Peyrou M, Vinciguerra M, Caillon A, Maeder C, Fournier M, Montet X, Rohner-Jeanrenaud F, Foti M. Chronic mTOR inhibition by rapamycin induces muscle insulin resistance despite weight loss in rats. Br J Pharmacol. 2012; 165:2325–40.
https://doi.org/10.1111/j.1476-5381.2011.01716.x
PMID:22014210

53. Houde VP, Brûlé S, Festuccia WT, Blanchard PG, Bellmann K, Deshaies Y, Marette A. Chronic rapamycin treatment causes glucose intolerance and hyperlipidemia by upregulating hepatic gluconeogenesis and impairing lipid deposition in adipose tissue. Diabetes. 2010; 59:1338–48.
https://doi.org/10.2337/db09-1324
PMID:20299475

54. Kennedy A, Webb CD, Hill AA, Gruen ML, Jackson LG, Hasty AH. Loss of CCR5 results in glucose intolerance in diet-induced obese mice. Am J Physiol Endocrinol Metab. 2013; 305:E897–906.
https://doi.org/10.1152/ajpendo.00177.2013
PMID:23941876

SUPPLEMENTARY MATERIALS

Supplementary Tables

Supplementary Table 1. List of primers used by SybrGreen for real-time PCR.

Name	Gene symbol	Primers sequence
Glyceraldehide 3-phoshate dehydrogenase	**GAPDH**	Sense: 5´-CATGTTCCAGTATGACTCCACTC-3´ Antisense: 5´-GGCCTCACCCCATTTGATGT-3´
Interleukin-6	**IL-6**	Sense: 5´-ATGGATGCTACCAAACTGGAT-3´ Antisense: 5´-TGAAGGACTCTGGCTTTGTCT-3´
Interleukin-1 beta	**IL-1β**	Sense: 5′-CTGAACTCAACTGTGAAATGCCA-3′ Antisense: 5′-AAAGGTTTGGAAGCAGCCCT-3´
Tumor necrosis factor- α	**TNF-α**	Sense 5´- ACGGCATGGA TCTCAAAGAC-3´ Antisense 5´- AGATAGCAAATCGGCT GACG-3´
Interleukin-18	**IL-18**	Sense: 5´- GACTCTTGCGTCAACTTCAAGG -3´ Antisense: 5´- CAGGCTGTCTTTTGTCAACGA -3´
Chemokine receptor type 5	**CCR5**	Sense: 5´-CGAAAACACATGGTCAAACG-3´ Antisense: 5´-TTCCTACTCCCAAGCTGCAT-3´
Chemokine ligand 5 (RANTES)	**CCL5**	Sense: 5´-ATATGGCTCGGACACCACTC-3´ Antisense: 5´-GTGACAAACACGACTGCAAGA -3´
Mammalian target of Rapamycin	**mTOR**	Sense: 5´- CTGGGACTCAAATCTCTCCAGTTC-3´ Antisense: 5´- GAACAATAGGGTGAATGATCCGGG-3´
Caspase-3	**Caspase-3**	Sense: 5´-ATGGGAGCAAGTCAGTGGAC-3´ Antisense: 5´-CGTACCAGAGCGAGATGACA-3´
Insuline receptor substrate-1	**IRS-1**	Sense: 5´- CCAGCCTGGCTATTTAGCTG-3´ Antisense: 5´-CCCAACTCAACTCCACCACT-3´
Insuline receptor substrate-2	**IRS-2**	Sense: 5´-GTAGTTCAGGTCGCCTCTGC-3´ Antisense: 5´-CAGCTATTGGGACCACCACT-3´
NAD-dependent protein deacetylase sirtuin-1	**SIRT-1**	Sense: 5´- AGTTCCAGCCGTCTCTGTGT-3´ Antisense: 5´- CTCCACGAACAGCTTCACAA-3´
NAD-dependent protein deacetylase sirtuin-3	**SIRT-3**	Sense: 5´ GCTGCTTCTGCGGCTCTATAC-3´ Antisense: 5´-GAAGGACCTTCGACAGACCGT-3´
NAD-dependent protein deacetylase sirtuin-6	**SIRT-6**	Sense: 5´- CTGAGAGACACCATTCTGGACT-3´ Antisense: 5´- GGTTGCAGGTTGACAATGACC-3´
Nuclear factor NF-kappa-B p105 subunit	**NFkB1**	Sense: 5´-GAAATTCCTGATCCAGACAAAAAC-3´Antisense: 5´-ATCACTTCAATGGCCTCTGTGTAG-3´
Nuclear factor NF-kappa-B p100 subunit	**NFkB2**	Sense: 5´-CTGGTGGACACATACAGGAAGAC-3´Antisense: 5´-ATAGGCACTGTCTTCTTTCACCTC-3´

Supplementary Table 2. Details of the ELISA assay methods.

Biomarker	Procedure	Sensitivity minimum Detectable dose (MDD)	Commercial producer
IL-1β	Quantikine® ELISA	0.46-4.80 pg/ml (The mean was 2.31 pg/ml)	R&D Systems
IL-6	Quantikine® ELISA	1.3-1.8 pg/ml (The mean was 1.6 pg/ml)	R&D Systems
TNF-α	Quantikine® ELISA	0.36-7.21 pg/ml (The mean was 1.88 pg/ml)	R&D Systems
Myostatin	Quantikine® ELISA	0.922-5.32 pg/ml (The mean was 2.25 pg/ml)	R&D Systems

Abbreviations: 1 IL-1β = interleukin 1β; IL6 = interleukin 6; TNF-α = Tumor necrosis factor alpha.

Supplementary Table 3. Kinases detected in this study.

Antibody used	Commercial Producer	Molecular weight of the protein
Anti-AMPK antibody	Abcam, Cambridge, MA, USA |(Cat. No. 80039)	62 kDa
Anti-AMPK (phospho Thr 172) antibody	Cell Signaling, Danvers, MA (Cat. No. 109458)	60 kDa
Anti-AKT antibody	Cell Signaling, Danvers, MA (Cat. No. 9272)	60 kDa
Anti- AKT (phospho S473) antibody	Abcam, Cambridge, MA, USA (Cat No. 81283)	56 kDa
Anti-NF-kb p65 antibody	Abcam, Cambridge, MA, USA (Cat No. 16502)	64 kDa
Anti NF-kb p65 (phospho S529) antibody	Abcam, Cambridge, MA, USA (Cat No. 16502)	60 kDa
mTOR	Cell Signaling, Danvers, MA (Cat. No. 2983T)	289 kDa
Anti-mTOR (phospho S2448) antibody	Abcam, Cambridge, MA, USA (Cat No. 109268)	kDa
Anti-SIRT1 antibody	Abcam, Cambridge, MA, USA (Cat No. 32441)	110 kDa
Anti-SIRT3 antibody	Abcam, Cambridge, MA, USA (Cat No. 217319) 28 kDa	
Anti-SIRT6 antibody	Abcam, Cambridge, MA, USA (Cat No. 191385) 39 kDa	
Anti-IRS1 antibody	Abcam, Cambridge, MA, USA (Cat No. 40777) 170 kDa	
Anti-IRS2 antibody	Abcam, Cambridge, MA, USA (Cat No. 134101) 137 kDa	
Anti-pro Caspase-3 antibody	Abcam, Cambridge, MA, USA (Cat No. 32150)	35 kDa
Anti-GAPDH antibody	Thermo Fisher Scientific, Waltham, MA (Cat. No. AM4300)	37 kDa